Supporting Online Material

Materials and Methods

Plasmids. A plasmid expressing EboV GP Zaire (Mayinga strain) was generated by subcloning the GP open reading frame from plasmid pCB6-GP (*1*) (a kind gift of P. Bates, University of Pennsylvania) into the pcDNA3.1-(Zeo) vector (Invitrogen, Carlsbad). pcDNA3.1-GPΔMuc, which lacks residues 309-489 in GP, was engineered as described (*2*). Plasmids expressing VSV G (*3*), CatL (*4*) and CatB (*4*) (kindly provided by T.S. Dermody, Vanderbilt University) have been described.

Cell lines and antibodies. Vero and 293T cells were maintained in Dulbecco's Modified Eagle's Medium (DMEM; Invitrogen) supplemented with 10% fetal bovine serum (Hyclone, Logan). MEFs derived from wild-type and $CatB^{-/-}$ $CatL^{+/+}$ mice (kindly provided by T.S. Dermody) have been described previously (*5*). MEFs derived from $CatB^{-/-}$ $CatL^{-/-}$ mice (*6*) were kindly provided by N. Fehrenbacher. EboV GP was detected by immunoblotting with a GP/sGP-specific antiserum kindly provided by A. Sanchez (Centers for Disease Control, Atlanta) (1:20000 dilution). Immunoblots were probed with secondary antibodies conjugated to horseradish peroxidase (1:5000 dilution) (Sigma), and developed using an enhanced chemiluminescence protocol (Perkin Elmer, Wellesley).

Construction of VSVΔG-GFP recombinant virus. A VSV cDNA lacking the G gene (pVSVΔG) was generated from plasmids encoding VSV recombinants MIG and GIL (*7*). This recombinant plasmid contained a 65-nt sequence comprising the VSV gene

start and end sequences flanking a stuffer sequence in place of the G gene. The green fluorescent protein (GFP) ORF was amplified from pGreenLantern (Invitrogen) and inserted between the leader and N genes of VSV by cloning into pVSV(+)41 (*8*), to generate pVSV1(+)-GFP. Plasmids pVSVΔG and pVSV1(+)-GFP were used to generate pVSVΔG-GFP using standard cloning techniques. Virus was recovered, amplified, and purified as described (*9*), except that a plasmid expressing VSV G was transfected into cells at each passage.

VSV pseudotypes. Viruses bearing VSV G, EboV GP, or EboV GPΔMuc were generated essentially as described (*10*). Briefly, 293T cells were transfected with a plasmid expressing an envelope glycoprotein, using Lipofectamine 2000 (Invitrogen). After 36–48 hours, cells were exposed to VSVΔG-GFP virus pseudotyped with VSV G (~1 Vero cell infectious unit [iu]/cell) for 1 h at 37˚C. Cells were washed to remove unbound virus, and infection was allowed to proceed for 24–36 h at 37˚C. Virus-containing supernatants were then harvested, concentrated by pelleting twice through a 10% sucrose cushion, resuspended in NTE buffer (10 mM Tris.Cl [pH 7.5], 135 mM NaCl, 1 mM EDTA), and frozen in aliquots at –80˚C. Experiments reported in Fig. 1–2 were performed with VSV-GPΔMuc rather than VSV-GP because the former were ~100-fold more infectious, and provided greater sensitivity over the background level of VSV G-dependent infectivity (~10^4 vs. ~10^2, respectively). Typical titers for VSV-GPΔMuc and VSV-GP in crude tissue-culture supernatants were 1×10^8 iu/ml and 1×10^6 iu/ml, respectively. Key findings were subsequently reproduced with pseudotypes bearing GP (Figs. S1–S5) and indicate no determinative role for the variable/mucin-like domain in

requirements for endosomal cysteine proteases in Vero cells, or in susceptibility to proteolytic processing in vitro.

Infectivity measurements in Vero cells. Infectivities of VSV pseudotypes in Vero cells were determined by exposing Vero monolayers to serial dilutions of virus and counting GFP-positive cells under a fluorescence microscope at 16–24 hours post-infection. Infectivity values are reported as iu/ml, where one iu corresponds to one GFP-positive cell. 20 to 200 cells were counted to obtain each measurement. Prior to infectivity measurement, VSV-GP was incubated with a VSV G-specific neutralizing monoclonal antibody (*11*) (100 μg/ml) for 30 min at room temp to reduce background infection. Relative infectivities of VSV pseudotypes in Figs. 1A,B and 2 and S1–S5 were determined by the following formula:

$$\text{Relative infectivity (\% iu/ml)} = [\text{iu/ml}_{\text{sample}} / \text{iu/ml}_{\text{mock treated virus in untreated cells}}] \times 100\%$$

Protease inhibitor experiments with VSV pseudotypes. Protease inhibitors E-64d, CA074, pepstatin A, aprotinin (Sigma, St. Louis), and FYdmk (*Z*-Phe-Tyr-(*t*Bu)-diazomethylketone; Calbiochem, San Diego) were dissolved in water (aprotinin) or dimethylsulfoxide (DMSO), and dispensed into culture medium containing 1% DMSO immediately before use. Cell monolayers in 24- or 48-well tissue culture plates were preincubated with inhibitors for 3 to 4.5 hours at 37˚C. VSV pseudotypes were then added directly to the culture medium containing DMSO/inhibitor, and infectivities were measured 16–24 hours later by counting GFP-positive cells and reported as described above. In some experiments, infection was monitored at both 24 and 48 hours post-

infection, but no appreciable increase in the number of GFP-positive cells was observed between 24 and 48 hours post-infection.

Infectivity measurements in MEFs. Infectivity of VSV-GPΔMuc in MEFs was determined by counting GFP-positive cells by flow cytometry using a FacScan instrument (BD, San José). To measure the capacities of CatB and/or CatL to enhance infection in MEFs in Fig. 1C,D, confluent cell monolayers in 12-well tissue culture plates were cotransfected with 0.8 μg of plasmid DNAs encoding β-gal, or CatB and/or CatL, and 0.8 μg plasmid DNA encoding monomeric red fluorescent protein (mRFP), using Lipofectamine 2000. Cells were exposed to virus 24 hours after transfection, and the percentage of infected cells (i.e., GFP-positive and mRFP-positive) in the transfected cell population (i.e., RFP-positive) was determined by two-color flow cytometry at 24 hours post-infection. At least 2000 cells RFP-positive cells were examined in each sample.

EboV infections. Experiments with infectious EboV were carried out under BSL-4 containment at the United States Army Medical Institute of Infectious Diseases (Fort Detrick, MD). Vero cells were pretreated with E-64d (300 μM) or CA074 (80 μM) in DMEM containing 1% DMSO for 4 hours, and then exposed to EboV-Zaire (1995 strain) (1 pfu/cell) (*12*) for 1 hour in the presence of inhibitor. Cultures were then washed thoroughly, and incubated with growth medium at 37˚C. At the indicated times, supernatants and cells were both harvested. Infectious virus in the supernatants was titrated by plaque assay as described (*13*). To measure levels of cell-associated viral proteins, we lysed cells with NP40 buffer (10 mM Tris.Cl [pH 7.5], 150 mM NaCl, 1%

NP40), and subjected postnuclear supernatants to SDS-PAGE and immunoblotting with EboV GP-specific antibody (see above). β-actin was used as a loading control.

Enzyme assays. The enzymatic activities of CatB and CatL in acidified lysates of Vero cells and MEFs were assayed with fluorogenic peptide substrates *Z*-Arg-Arg-AMC (Calbiochem) and (*Z*-Phe-Arg)$_2$-R110 (Molecular Probes, Eugene), respectively, as described (*4*), except that lysates were pretreated with 1 μM FYdmk or 1 μM CA074 for 20 min at room temperature prior to assaying for CatB or CatL, respectively. These assay conditions were validated for specificity using purified CatB and CatL (Calbiochem). The lack of CatB activity in *CatB*$^{-/-}$ *CatL*$^{+/+}$ MEFs and the presence of similar levels of CatL activity in *CatB*$^{-/-}$ *CatL*$^{+/+}$ and wild-type MEFs was confirmed as described above.

In vitro protease treatments. Pelleted VSV preparations (0.5 to 2 μg protein) were incubated with no enzyme (mock), or purified CatB and/or CatL in acetate buffer (100 mM sodium acetate [pH 5.5], 1 mM EDTA, 5 mM DTT) at 37˚C, and reactions were terminated by removal onto ice, addition of 50 μM E-64 (Sigma), and neutralization with 100 mM Hepes [pH 7.4]. VSV particles were diluted into DMEM prior to infection. Prior to analysis of EboV GP by SDS-PAGE and immunoblotting, samples were treated with protein N-glycosidase F (New England Biolabs, Beverly) to remove N-linked oligosaccharides, unless otherwise mentioned.

Supporting Online Text

Cleavage of EboV GPΔMuc (Figs. 2 and S3) and GP (Fig. S3) within VSV particles by purified CatL resulted in an ~18 kDa GP1 fragment ($GP1_{18K}$) that remained associated with viral particles (Fig. S4). No smaller fragments were detected with the polyclonal anti-GP antiserum. These findings strongly suggest that C-terminal sequences of GP1, including GP1 residues 309–489 comprising the variable/mucin-like domain (Muc), are extensively cleaved during the GP1→$GP1_{18K}$ step. They suggest also that $GP1_{18K}$ is an N-terminal fragment of GP1 (see below).

In mature GP1-GP2 trimers, GP1 is disulfide-bonded to GP2 via residues Cys 53 (GP1) and Cys 609 (GP2) (*2*). As a consequence, dissociation of GP1 from viral particles requires reduction (*14*). We found that $GP1_{18K}$ retains this property (Fig. S4), indicating that it remains disulfide-bonded to GP2, and confirming that $GP1_{18K}$ is an N-terminal fragment of GP1 that contains Cys 53.

EboV GP can be unambiguously classified as a type I viral glycoprotein by virtue of its similarities to other type I glycoproteins in sequence, overall organization, and structure (e.g., see (*15*)). Viral inactivation due to premature deployment of the membrane fusion machinery following in vitro exposure to the triggering signal is a hallmark of type I viral glycoproteins (*16, 17*). We propose that VSV-GPΔMuc inactivation by CatB digestion of $GP1_{18K}$ reflects premature deployment of GP2 in an analogous manner. The properties of $GP1_{18K}$ are consistent with its proposed role as a glycoprotein clamp that regulates the GP2 membrane fusion machinery: it contains the

most highly conserved GP1 amino acid sequences and structural features, including the intrasubunit and intersubunit disulfide bonds (two and one, respectively) *(2)*. Initial attempts to recapitulate EboV $GP1_{18K}$-dependent cell membrane fusion with purified CatB at pH 5.5 were confounded by the cytotoxicity of the extracellular enzyme, indicating a need for additional approaches to determine whether CatB is not only necessary but also sufficient for triggering of EboV membrane fusion within the acidic endosomal milieu of target cells.

Supporting Figure Legends and Table Captions

Fig. S1. Activity of endosomal cysteine proteases is necessary for EboV GP-dependent infection of Vero cells. **(A)** Effects of class-specific protease inhibitors on infectivities (iu/ml) of VSV-G, VSV-GP, or VSV-GPΔMuc. DMSO vehicle (1%) (none), aprotinin (500 μg/ml), pepstatin A (200 μM), E-64d (300 μM). Error bars, S.D from three replicates.

Fig. S2. Activity of endosomal cysteine protease CatB is necessary for EboV GP-dependent infection of Vero cells. Effect of CatB-selective inhibitor CA074 (left) and CatL-selective inhibitor FYdmk (right) on infectivity of VSV-GP. Averages from duplicate experiments are shown.

Fig. S3. Purified CatL cleaves both EboV GP and GPΔMuc to generate $GP1_{18K}$. VSV-GP and VSV-GPΔMuc were incubated with the indicated concentration of CatL for 1 hour at pH 5.5 and 37˚C, and samples were subjected to SDS-PAGE and immunoblotting to detect GP1.

Fig. S4. EboV $GP1_{18K}$ is an N–terminal fragment of GP1 that remains covalently associated to GP2 via the GP1(Cys 53)–GP2(Cys 609) disulfide bond. **(A)** Schematic diagram of experimental approach to separate VSV particle-associated and released proteins. **(B)** VSV particles (2 μg) containing $GP1_{18K}$ derived from GP (top) or GPΔMuc (bottom) by incubation with 10 μg/ml CatL for 1 hour at pH 5.5 and 37˚C were incubated with urea (6M) or urea and DTT (100 mM) for 30 min at 37˚C. Samples were then

overlaid onto a 25% sucrose cushion (0.5 ml). Viral particles were pelleted in a TLA100 rotor (Beckman) at 75000 rpm and 4˚C for 1 hour. The cushion was fractionated, and three fractions from the top (T) and one fraction from the bottom (B) were subjected to SDS-PAGE and immunoblotting to detect GP1. Samples were not treated with protein N-glycosidase F prior to SDS-PAGE.

Fig. S5. VSV particles containing $GP1_{18K}$ derived from EboV GP1 bypass a block to GP1 cleavage in Vero cells. Cells were treated with inhibitors to obtain the approximate levels of cellular CatB (*B%*) and CatL (*L%*) activities shown to the right of the bars. (*B 100% L 100%)*, no drug. (*B 10% L 0%)*, 10 μM FYdmk. (*B 10% L 100%)*, 40 μM CA074. (*B 0% L 0%)*, 10 μM FYdmk + 40 μM CA074. Cells were then infected with VSV particles containing GP1 (GP1) or $GP1_{18K}$ (18K) (generated by incubation with 20 μg/ml CatL treatment for 1 hour at pH 5.5 and 37˚C). Results from two experiments are shown.

Chandran et al.
Fig. S1

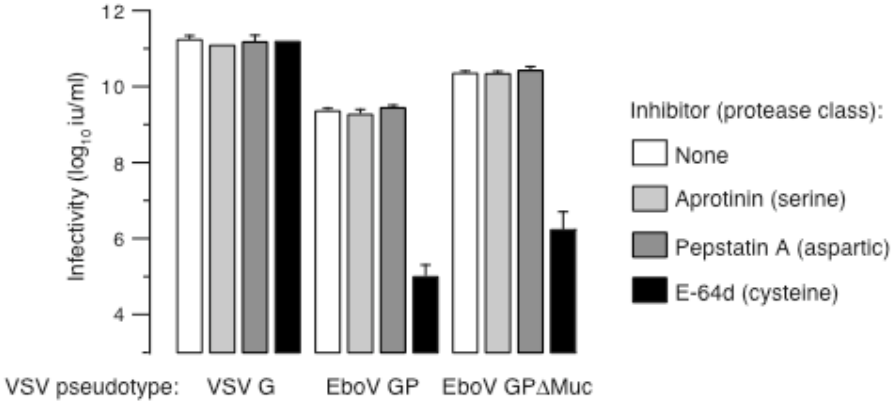

Chandran et al.
Fig. S2

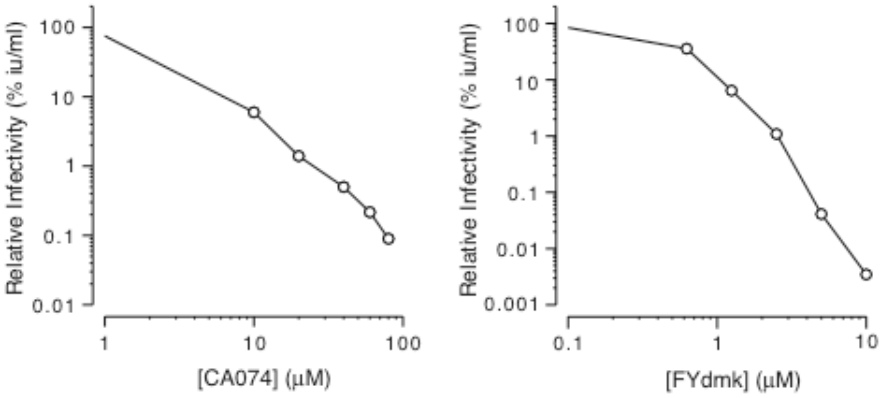

Chandran et al.
Fig. S3

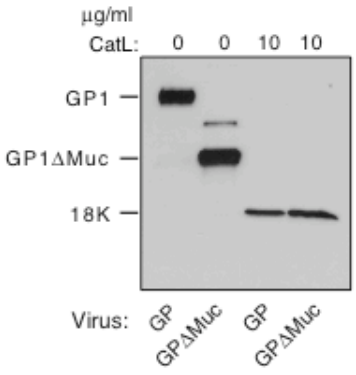

Chandran et al.
Fig. S4

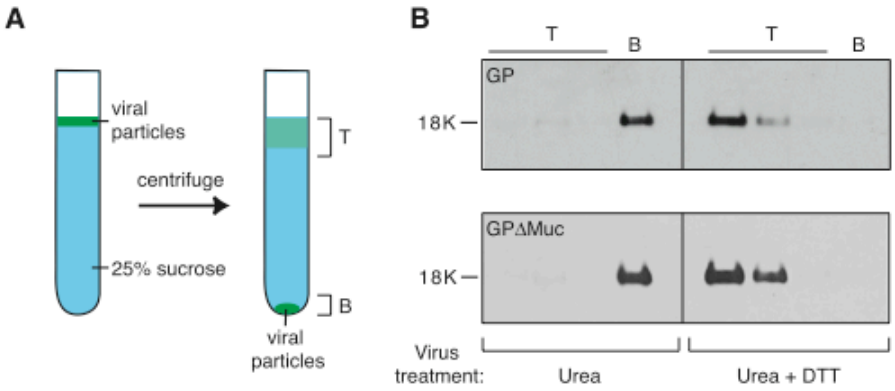

Chandran et al.
Fig. S5

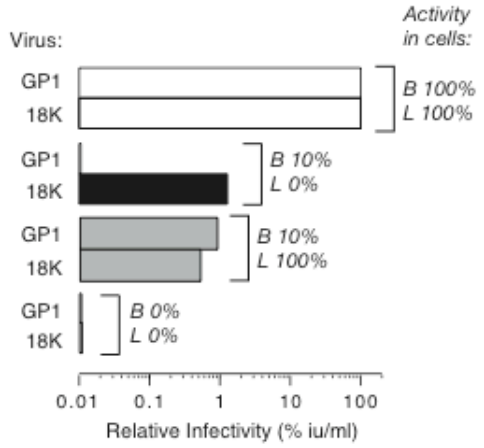

Table S1

Table S1. Relative susceptibility of VSV-GPΔMuc infection to FYdmk and CA074 reveals a role for CatL in EboV GP-dependent infection of Vero cells. CatB and CatL activities (% arbitrary units) were calculated relative to untreated cells (*18*) and are results from three experiments. Relative infectivity values (% iu/ml) from two experiments are shown.

Inhibitor (μM)	Enzyme activity (%) (± S.D.)		Relative infectivity (% iu/ml)
	CatB	CatL	
CA074 (40 μM)	10 ± 2 %	94 ± 1 %	1.3 %
			1.5 %
FYdmk (10 μM)	11 ± 2 %	0 ± 0 %	0.017 %
			0.015 %

References

1. R. J. Wool-Lewis, P. Bates, *J. Virol.* **72**, 3155 (1998).
2. S. A. Jeffers, D. A. Sanders, A. Sanchez, *J. Virol.* **76**, 12463 (2002).
3. L. Naldini, U. Blomer, F. H. Gage, D. Trono, I. M. Verma, *Proc. Natl. Acad. Sci. USA* **93**, 11382 (1996).
4. D. H. Ebert, J. Deussing, C. Peters, T. S. Dermody, *J. Biol. Chem.* **277**, 24609 (2002).
5. J. Deussing *et al.*, *Proc. Natl. Acad. Sci. USA* **95**, 4516 (1998).
6. U. Felbor *et al.*, *Proc Natl Acad Sci U S A* **99**, 7883 (2002).
7. G. W. Wertz, R. Moudy, L. A. Ball, *J. Virol.* **76**, 7642 (2002).
8. S. P. Whelan, J. N. Barr, G. W. Wertz, *J. Virol.* **74**, 8268 (2000).
9. S. P. Whelan, L. A. Ball, J. N. Barr, G. T. Wertz, *Proc. Natl. Acad. Sci. USA* **92**, 8388 (1995).
10. A. Takada *et al.*, *Proc. Natl. Acad. Sci. USA* **94**, 14764 (1997).
11. L. Lefrancios, D. S. Lyles, *Virology* **121**, 157 (1982).
12. P. B. Jahrling *et al.*, *J. Infect. Dis.* **179 Suppl 1**, S224 (1999).
13. N. K. Jaax *et al.*, *Arch. Pathol. Lab. Med.* **120**, 140 (1996).
14. R. J. Wool-Lewis, P. Bates, *J. Virol.* **73**, 1419 (1999).
15. W. Weissenhorn *et al.*, *Mol. Membr. Biol.* **16**, 3 (1999).
16. F. Boulay, R. W. Doms, I. Wilson, A. Helenius, *EMBO J.* **6**, 2643 (1987).
17. W. Mothes, A. L. Boerger, S. Narayan, J. M. Cunningham, J. A. Young, *Cell* **103**, 679 (2000).
18. Materials and methods are available as supporting material on *Science* Online.